

# Diagonal patterns and chevron effect in intersecting traffic flows

J. CIVIDINI<sup>1</sup> (a), C. APPERT-ROLLAND<sup>1</sup> (b) and H.J. HILHORST<sup>1</sup> (c)

<sup>1</sup> *Laboratoire de Physique Théorique, bâtiment 210  
Université Paris-Sud and CNRS, 91405 Orsay Cedex, France*

PACS 05.65.+b – Self-organized systems  
PACS 89.75.Kd – Patterns in complex systems  
PACS 45.70.Vn – Granular models of complex systems; traffic flow

**Abstract** – We study a lattice model of two perpendicular intersecting flows of pedestrians represented by hard core particles of two types, eastbound ( $\mathcal{E}$ ) and northbound ( $\mathcal{N}$ ). Each flow takes place on a strip of width  $M$  so that the intersection is an  $M \times M$  square lattice. In experiment and simulation there occurs on this square spontaneous formation of a diagonal pattern of alternating  $\mathcal{E}$  and  $\mathcal{N}$  particles. We show that this pattern formation may be understood in terms of a linear instability of the corresponding mean field equations. A refined investigation reveals that the pattern actually consists of chevrons rather than straight diagonals. We explain this effect as the consequence of the existence of a nonlinear mode sustained by the interaction between the two types of particles.

**P**edestrian motion in dense environments is of much theoretical and practical interest [1, 2]. Instances of applications are shopping streets, waiting lines, crowds that enter or leave a room, converge to a stadium, participate in a demonstration, and so on. Simplified models help us understand the behavior of individuals under such circumstances as well as the collective behavior that results from it. They may also exhibit phenomena of more fundamental interest for statistical physics.

The present investigation was motivated by the experimental observation [3] of an instability that occurs at the intersection of two perpendicular unidirectional flows of pedestrians: Walkers of the two types segregate into a pattern of approximately diagonal stripes that propagates as a running wave. In a variety of models simulating crossing flows (agent based [4, 5], PDEs [5], BML [6]) it has been remarked that such patterns occur, but the formation mechanism has not been systematically studied. In this paper we tackle this question with combined numerical and the-

oretical approaches. First, we explain the pattern formation instability both for closed and open systems from a linear stability analysis of the mean field equations. Moreover, we show that superposed on the instability there is a subtle ‘chevron effect’, and we identify a propagation mode that exhibits this chevron structure. This effect, which so far has not been observed, may be expected to be visible under favorable circumstances to be discussed in the conclusion.

We model a street of width  $M$  as a set of  $M$  parallel one-dimensional lattices or ‘lanes’ [7]. Two intersecting one-way streets lead to the geometry of fig. 1, which has the  $(1, 1)$  diagonal through the origin as an axis of symmetry. Eastbound (or  $\mathcal{E}$ ) and northbound (or  $\mathcal{N}$ ) particles are injected into each lane at some large distance  $L$  from the intersection square. An  $\mathcal{E}$  particle ( $\mathcal{N}$  particle) is allowed to hop only towards its neighboring site on the east (north), provided that site is empty. No lane changes or turns are allowed. The injection probability  $\alpha$  per time step determines the incoming current  $J(\alpha)$  in each lane [8]. For moving the particles we choose for convenience the frozen shuffle update [10]. It will appear that the phenomena of interest are independent of the details of the update

(a) E-mail: julien.cividini@th.u-psud.fr

(b) E-mail: cecile.appert-rolland@th.u-psud.fr

(c) E-mail: henk.hilhorst@th.u-psud.fr

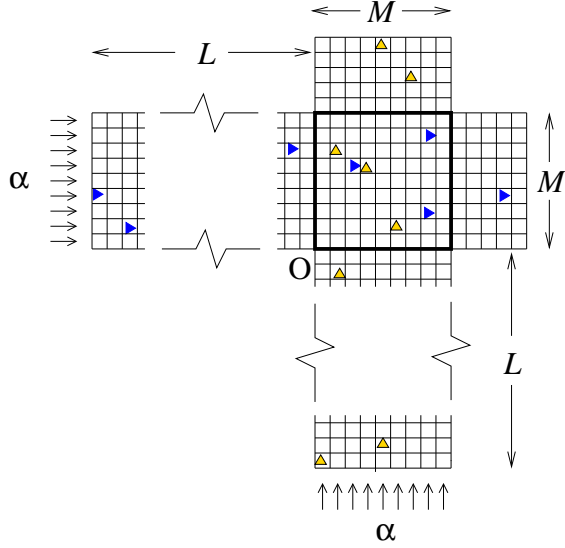


Fig. 1: Intersection of two one-way streets of width  $M$ . The blue particles ( $\blacktriangleright$ ) move eastward and the orange particles ( $\blacktriangle$ ) northward. The parameter  $\alpha$  determines the particle injection rate. The region bordered by the heavy solid line is the ‘intersection square’. Lane changes, whether in the incoming street segments or in the intersection square, are forbidden.

mechanism. Under frozen shuffle update, during a unit interval all particles are visited in a fixed sequence and each one executes a move unless its target site is occupied; that is, the particles move ballistically unless blocked. Particles entering the system are randomly inserted in the update sequence and those exiting are deleted from it. Blocking may happen to a particle either in the intersection square itself or in the street segments leading up to it. In the simulations we chose  $L$  (see fig.1) larger than the lengths of any waiting lines observed at the entrance, so that effectively  $L = \infty$ . We therefore have a simple model depending only on the two parameters  $\alpha$  and  $M$ , whose interest as an example of a driven nonequilibrium system goes, we believe, beyond the present application. Simulations were carried out for intersecting streets of widths up to  $M = 640$ . The pattern formation studied here appears in the so-called *free flow phase* ( $\alpha \lesssim 0.10$  for the  $M$  values concerned), in which in each lane the current through the intersection is equal to  $J(\alpha)$ . We stay away from higher values of  $\alpha$ , where jamming transitions are known to occur [7, 11, 12].

For  $t > 0$  particles start entering the initially empty intersection square. After a number of time steps typically no larger than a few times the linear lattice size  $M$ , the occupation of the intersection square reaches a stationary state. We observed that this state has the following

properties.

(i) There is an  $\alpha$  dependent penetration length  $\xi(\alpha)$ , such that for  $M \lesssim \xi$  the occupation of the intersection square appears disordered to the eye. For  $\alpha = 0.09$  the penetration length equals  $\xi(\alpha) \approx 50$ ; for  $\alpha \rightarrow 0$  it diverges as  $\sim \alpha^{-1}$ .

(ii) For  $M \gtrsim \xi$  alternating stripes of  $\mathcal{E}$  and  $\mathcal{N}$  particles parallel to the  $(1, -1)$  direction begin to be distinguishable. For  $M \gg \xi$  they are clearly visible, as may be seen from fig.2, where  $M = 640$  and  $\alpha = 0.09$ . The striped pattern propagates as a running wave, as is witnessed by fig.3 where a small region of the system is shown at an interval of ten time steps. Although the striped pattern never becomes fully regular, its wavelength is typically in the range from 5 to 15 lattice distances. This organization into stripes decreases the probability for a particle to be blocked below its value for a random particle distribution, and therefore increases the particles’ average velocity.

(iii) Closer examination of fig.2 reveals an effect just barely visible to the eye: the angle  $\theta$  of the striped pattern (as measured anticlockwise from the north) is *not exactly equal to*  $45^\circ$  but deviates from it by an amount  $\Delta\theta(\mathbf{r})$ , where  $\mathbf{r} = (x, y)$  denotes the position in space. Although small (of the order of a degree), the deviation  $\Delta\theta(\mathbf{r})$  may be measured unambiguously in the neighborhood of any site  $\mathbf{r}$ . It is positive above the axis of symmetry and negative below it.

(iv) In the triangular regions delimited by the dashed white lines in fig.2, the deviation  $\Delta\theta(\mathbf{r})$  is close to a constant which equals  $+\Delta\theta_0$  in the upper and  $-\Delta\theta_0$  in the lower triangle. This confers to the stripes the appearance of chevrons, and we will speak of the ‘chevron effect’. The tips of the chevrons, located in the transition zone between the two triangles, are rounded. Empirically we find  $\Delta\theta_0(\alpha) \simeq c\alpha$  with  $c \approx 15^\circ$ . The penetration length  $\xi$  is the characteristic scale after which  $\Delta\theta$  reaches its plateau value.

We will now first explain the stripe formation instability and then return to the chevron effect.

Let the occupation number  $n_t^X(\mathbf{r})$  be equal to 1 (to 0) if after time step  $t$  site  $\mathbf{r}$  is (is not) occupied by an  $X$  particle, where  $X = \mathcal{E}, \mathcal{N}$ . Let the densities  $\rho_t^{\mathcal{E}, \mathcal{N}}(\mathbf{r}) = \langle n_t^{\mathcal{E}, \mathcal{N}}(\mathbf{r}) \rangle$  be the averages over the stochastic boundary conditions. In an exact description of the time evolution these particle densities would couple to a hierarchy of higher order correlations. Instead, denoting basis vectors by  $\mathbf{e}_{x,y}$ , we postulate the mean-field equations

$$\begin{aligned} \rho_{t+1}^{\mathcal{E}}(\mathbf{r}) &= [1 - \rho_t^{\mathcal{N}}(\mathbf{r})]\rho_t^{\mathcal{E}}(\mathbf{r} - \mathbf{e}_x) + \rho_t^{\mathcal{N}}(\mathbf{r} + \mathbf{e}_x)\rho_t^{\mathcal{E}}(\mathbf{r}), \\ \rho_{t+1}^{\mathcal{N}}(\mathbf{r}) &= [1 - \rho_t^{\mathcal{E}}(\mathbf{r})]\rho_t^{\mathcal{N}}(\mathbf{r} - \mathbf{e}_y) + \rho_t^{\mathcal{E}}(\mathbf{r} + \mathbf{e}_y)\rho_t^{\mathcal{N}}(\mathbf{r}), \end{aligned} \quad (1)$$

in which the pair correlations  $\langle n^{\mathcal{E}} n^{\mathcal{N}} \rangle$  have been factorized and the interaction terms  $\langle n^X n^X \rangle$  between same-type

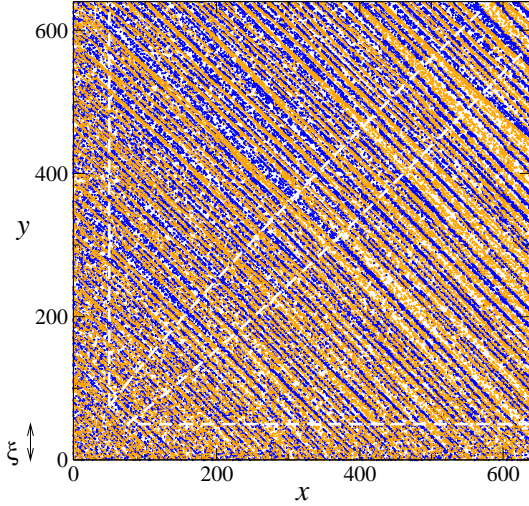


Fig. 2: Typical configuration of the intersection square in the stationary state for  $M = 640$  and  $\alpha = 0.09$ . The blue particles arrive from the left and the orange ones from the bottom. Between the lower-left and the upper-right, the particles self-organize to form a diagonal pattern. The dashed white lines delimit two triangular regions discussed in the text. Obtained for a particle system with frozen shuffle update.

particles have been neglected. When the nonlinear terms in these equations vanish, the two particle densities  $\rho_t^{\mathcal{E}}(\mathbf{r})$  and  $\rho_t^{\mathcal{N}}(\mathbf{r})$  travel eastward and northward, respectively, at unit speed; the nonlinear terms reduce this speed. Our neglect of the  $\mathcal{E}\mathcal{E}$  and  $\mathcal{N}\mathcal{N}$  interactions is justified as follows. In the limit where the typical density  $\bar{\rho}$  of the two particle types is low, the frequency of  $\mathcal{E}/\mathcal{N}$  and  $\mathcal{N}/\mathcal{E}$  blocking events is  $\sim \bar{\rho}^2$ , but that of same-type particle blocking is  $\sim \bar{\rho}^3$  because two successive same-type particles in the same lane both advance at unit speed and never obstruct each other unless there is interference by a third particle, of the other type, that crosses their lane. We have checked these proportionalities in our simulations.

The auxiliary problem in which eqs. (1) are solved on a torus explains the basic stripe formation instability. In this case the uniform state with  $\rho_t^{\mathcal{E},\mathcal{N}}(\mathbf{r}) = \bar{\rho}$  is a stationary solution. By a linear stability analysis for small deviations  $\delta\rho_t^{\mathcal{E},\mathcal{N}}(\mathbf{r}) = \rho_t^{\mathcal{E},\mathcal{N}}(\mathbf{r}) - \bar{\rho}$  we showed that there is an unstable Fourier mode traveling in the  $(1,1)$  direction and having wavelength  $\lambda_{\max} = 3\sqrt{2}[1 - (\sqrt{3}/\pi)\bar{\rho}] + \mathcal{O}(\bar{\rho}^2)$ . This calculation therefore explains the formation of a diagonal striped pattern.

The nonlinear regime on the torus is beyond analytic study; however, numerical solution of eqs. (1), still with toroidal boundary conditions, shows that the system tends to a stationary state consisting of stripes with alternat-

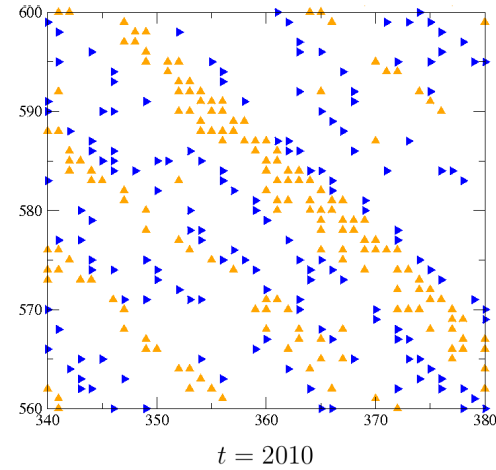
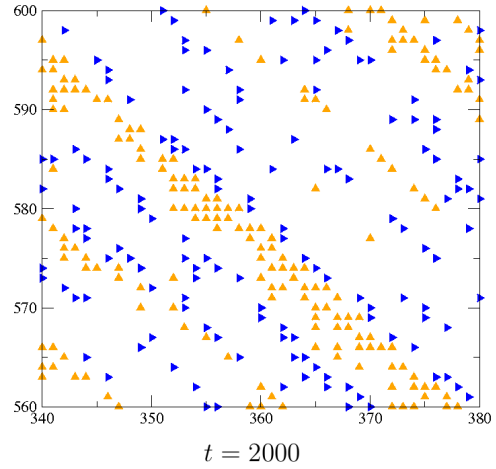


Fig. 3: Two snapshots of part of a system similar to Fig. 2, taken at an interval of 10 time steps in the upper triangular region. The particles enter the interaction square randomly and independently. On their way through the square they get organized into stripes that gradually become very compact, as frozen shuffle update permits the existence of particles following each other and moving as a whole. The orange particles have traveled a longer distance through the square ( $y \approx 580$ ) than the blue particles did ( $x \approx 360$ ), and therefore show a higher degree of compactification. Blue stripes move to the right and orange stripes to the north, resulting in an overall pattern moving in the  $(1,1)$  direction.

ingly only  $\rho_t^{\mathcal{E}}(\mathbf{r}) \neq 0$  or only  $\rho_t^{\mathcal{N}}(\mathbf{r}) \neq 0$ , and separated by unoccupied sites in such a way that the nonlinear terms in (1) vanish at all times.

The crossing street system that motivates this work has the open boundary conditions of fig. 1. When passing from that particle model to the nonlinear mean field equations

(1) we simultaneously simplify these boundary conditions and replace them with the time dependent stochastic ones

$$\begin{aligned} \rho_t^{\mathcal{E}}(0, k) &= \eta_t^{\mathcal{E}}(k), & \rho_t^{\mathcal{N}}(k, 0) &= \eta_t^{\mathcal{N}}(k), \\ \rho_t^{\mathcal{E}}(M+1, k) &= 0, & \rho_t^{\mathcal{N}}(k, M+1) &= 0, \end{aligned} \quad (2)$$

for all  $k = 1, 2, \dots, M$ , where the  $\eta_t^{\mathcal{E}, \mathcal{N}}(k)$  are i.i.d. random variables of average  $\bar{\eta}$ . The details of their distribution are unimportant and we have chosen a uniform distribution on  $[\frac{1}{2}\bar{\eta}, \frac{3}{2}\bar{\eta}]$ . Here  $\bar{\eta}$  replaces  $\alpha$  as the control parameter. The initial condition is arbitrary. It is now necessary to show that this boundary noise excites unstable modes analogous to those found above for the torus.

First, eqs. (1) and (2) may again be linearized. Their Green function, which expresses the effect of a unit perturbation confined to a single border site at a single instant of time, is a nonrandom object. Its analytic derivation is very long and technical; it will be the subject of a future publication. However it may also be calculated numerically exactly from the linearized equations. This calculation shows that the initial perturbation propagates in the  $(1, 1)$  direction, spreads out within a smooth envelope of width  $\sim \sqrt{t}$ , and develops oscillations having a wavelength of a few lattice units and traveling at a phase velocity different from the speed of the peak. The oscillations are of constant phase along any straight line perpendicular to the  $(1, 1)$  direction, which means, that the stripes are at exactly  $45^\circ$ . This demonstrates the pattern formation instability in the case of open boundaries. However, we have found no sign of the chevron effect in this linearized solution.

By contrast, numerical resolution of the full nonlinear equations (1) with (2) leads to the same chevron effect as simulation of the particle system. An important conclusion is therefore that this effect is not due to the specifics of the particle model, of the boundary conditions (as long as they are open) and/or of the update procedure, but appears to be generic.

We now pursue our observations on the particle system after it has reached a stationary state.

(v) The stripes of the  $\mathcal{E}$  and the  $\mathcal{N}$  particles move almost without any mutual penetration. This is compatible with a slope  $\theta$  of the stripes only if  $\tan \theta(\mathbf{r}) = v^{\mathcal{E}}(\mathbf{r})/v^{\mathcal{N}}(\mathbf{r})$ , where  $v^{\mathcal{E}, \mathcal{N}}$  is the average stationary state velocity of the  $\mathcal{E}, \mathcal{N}$  particles on site  $\mathbf{r}$ . Since the boundary conditions impose the same stationary current  $J$  in each lane, we have  $J = \rho^{\mathcal{E}}(\mathbf{r})v^{\mathcal{E}}(\mathbf{r}) = \rho^{\mathcal{N}}(\mathbf{r})v^{\mathcal{N}}(\mathbf{r})$  with  $\rho^{\mathcal{E}, \mathcal{N}}(\mathbf{r})$  the stationary state densities. Combined with the equation for  $\tan \theta(\mathbf{r})$  this yields

$$\tan \theta(\mathbf{r}) = \rho^{\mathcal{N}}(\mathbf{r})/\rho^{\mathcal{E}}(\mathbf{r}). \quad (3)$$

It follows from (3) that  $\Delta \theta(\mathbf{r}) \neq 0$  requires  $\rho^{\mathcal{E}}(\mathbf{r}) \neq \rho^{\mathcal{N}}(\mathbf{r})$ , which, we note, is not forbidden by symmetry and was

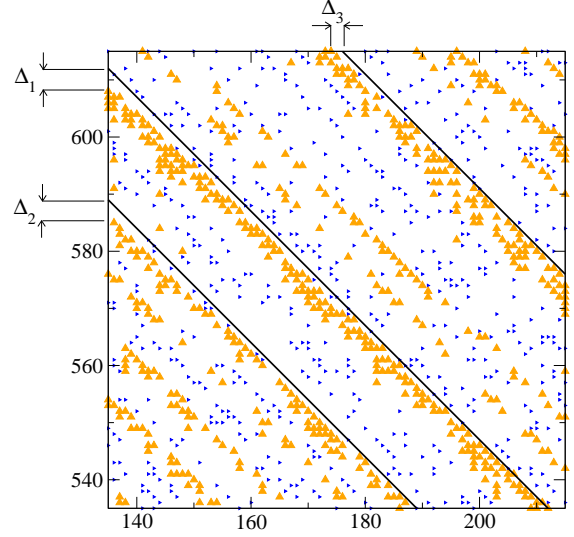


Fig. 4: Zoom on a region of fig. 2. To emphasize their difference the northbound particles ( $\blacktriangle$ ) have been indicated by larger symbols than the eastbound particles ( $\blacktriangleright$ ). The black solid lines are at an angle of  $45^\circ$ . The nonzero distances  $\Delta_1, \Delta_2$ , and  $\Delta_3$  show that locally  $\Delta \theta(\mathbf{r}) > 0$ .

checked numerically both in the simulations of the particle system and in the numerical solution of (1) with (2). This establishes the general consistency of the picture, still without explaining it.

(vi) Next we refer to the zoom, shown in fig. 4, on an area located in the upper triangular region of fig. 2. We observe that in this region the stripes of the  $\mathcal{N}$  particles are dense, whereas those of the  $\mathcal{E}$  particles are sparse. A consequence, visible even if barely so, is that the upper triangular region in fig. 2 looks bluish and the lower triangle more orange-like. The asymmetry observed here between the two particle types, which is also present in fig. 3, will offer the clue to understand the chevron effect.

The core of the problem is to show the existence of modes of propagation having stripe angles different from  $45^\circ$ . We will exhibit such a mode, that will be realized approximately near the entrance boundary of the  $\mathcal{E}$  particles, that is, for  $x \approx \xi$  but  $y \gg \xi$ . Close to this boundary the  $\mathcal{E}$  particles ( $\blacktriangleright$ ), having entered the intersection square randomly, fill the space offered to them between the  $\mathcal{N}$  stripes ( $\blacktriangle$ ). This suggests to consider the special class of  $\mathcal{N}$  stripes of which an example is shown in fig. 5a. The stripes consist of ‘concatenations’ of diagonal segments at an angle of  $45^\circ$ , connected by ‘kinks’ such as the one that occurs in fig. 5a at the level of particle B, and that is associated with the presence of the eastbound particle A. The other  $\mathcal{E}$  particles in fig. 5a occupy random positions. For

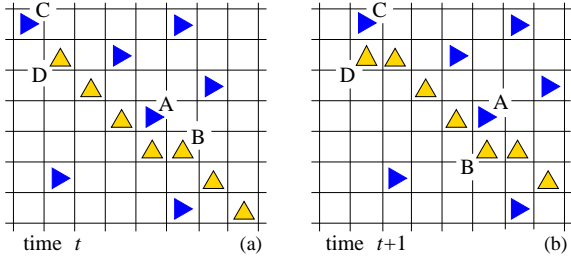


Fig. 5: Mechanism causing the deviation  $\Delta\theta$  of a stripe of northbound particles (▲) in the upper triangular region.

ease of analysis we now invoke the irrelevance of the details of the time evolution rules and employ in the present argument the alternating parallel update: at each time step first all  $\mathcal{E}$  particles move simultaneously (unless blocked) and then all  $\mathcal{N}$  particles do so.

When this update procedure is applied to the configuration of fig. 5a, we see that during the  $(t+1)$ th time step none of the eastbound particles is blocked; in particular, A and C move and block B and D, respectively. As a result the kink associated with A moves one step to the right along the northbound stripe, and C creates a new kink at the beginning of the stripe, at the level of particle D (see fig. 5b). In the next time steps particles A and C will both travel from left to right along the stripe, each of them taking its associated kink along, and the connected structure of the stripe will be preserved.

If the set of kinks has a linear density  $\rho_{\text{kink}}$  along the stripe, the average stripe angle  $\theta$  will be given by  $\tan\theta = (1 - \rho_{\text{kink}})^{-1}$ . Since  $\rho_{\text{kink}}$  also represents the fraction of blocked moves of the  $\mathcal{N}$  particles, the stripe's speed will be  $v^{\mathcal{N}} = 1 - \rho_{\text{kink}}$ . Hence we have demonstrated the most distinctive ingredient of the chevron effect: the existence of a nonlinear mode consisting of a stripe with an average slope different from  $45^\circ$ , that propagates at an average speed  $v^{\mathcal{N}} < 1$ .

The snapshot shown in fig. 6 demonstrates that this mode arises spontaneously in a Monte Carlo time evolution. The simulation was carried out with alternating parallel update. The particles enter the intersection randomly. They then self-organize into diagonal stripes with kinks. In fig. 6, red lines identify examples of concatenations with kinks similar to those considered in fig. 5. The angle  $\theta(\mathbf{r})$  in such relatively small systems arises only as an average performed over a sufficiently long measuring time in the stationary state.

Similar modes will be present for a wide class of time evolution rules, including those of the original particle system with frozen shuffle update, and those of eqs. (1);

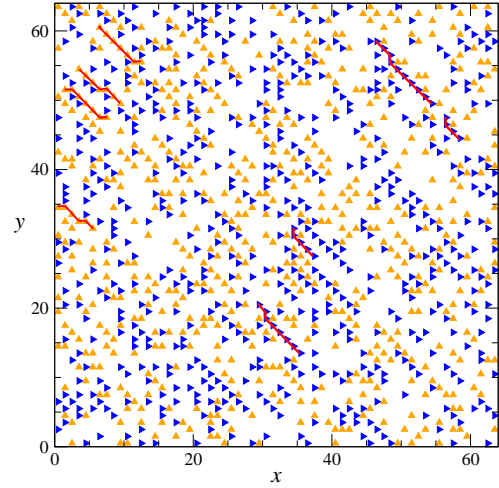


Fig. 6: Snapshot of the particles in an intersection square of linear dimension  $M = 64$ . The blue ones (▶) move eastward and the orange ones (▲) upward. Red lines identify examples of concatenations with kinks of the kind studied in fig. 4 of the Letter. This snapshot was obtained for a particle system with  $\alpha = 0.15$  and alternating parallel update; it was taken just after the move of the (blue)  $\mathcal{E}$  particles.

for both of these the explicit analysis would, however, be much more difficult. Of course quantitative features such as the exact value of  $\Delta\theta$  or the wavelength of the pattern will depend on the specifics of the time evolution rules.

Returning to the example of fig. 5 we note that a uniformly random spatial distribution of the  $\mathcal{E}$  particles would lead to  $\rho_{\text{kink}} = \rho^{\mathcal{E}}$ , and that  $v^{\mathcal{E}} = 1$ . If we assume that these expressions can also be used for the full problem, we are led to a fully explicit expression for the angle, namely  $\tan\theta = (1 - J)^{-1}$ , in which  $J(\alpha)$  is known [8]. Since a correlated distribution of the  $\mathcal{E}$  particles (e.g. if  $\mathcal{E}$  particles would themselves tend to be organized into stripes) would lead to a lower  $\rho_{\text{kink}}$ , we expect that this formula, while giving the correct order of magnitude, overestimates the inclination. Indeed, for  $J = 0.06$  it yields  $\Delta\theta_0 = 1.8^\circ$ , to be compared to  $0.7^\circ$  obtained via eq. (3) and  $0.9^\circ$  from direct measurement, both in a frozen shuffle update simulation.

We have presented a combination of simulations, numerical work, and analytic results that, first, explain the stripe formation instability observed in real traffic, and secondly, show that it is accompanied by a subtle but unmistakable ‘chevron’ effect, quantified by an angular deviation  $\Delta\theta(\mathbf{r})$ . A detailed account is in preparation [13, 14]. We found that fully developed stripes and chevrons exist only for linear lattice sizes  $M \gg \xi$ . Since  $\xi \sim \alpha^{-1} \sim \rho^{-1}$ , it follows that, equivalently, stripe and chevron formation

is subject to the requirement  $g \equiv \rho M \gg 1$ . Here  $g$  represents the mean number of encounters made by a particle during its traversal of the intersection square with perpendicularly traveling particles; therefore  $g$  is the effective coupling constant governing the pattern formation. Whereas in the present study we achieve  $g \gg 1$  by compensating a small  $\rho$  by a very large  $M$ , the same requirement is fulfilled in experiments and realistic agent based models [3–5] by the product of a larger  $\rho$  and moderate  $M$ . Because of its smallness, observing the chevron effect in an experiment or in a real-life traffic situation will necessarily require statistical averaging over a large amount of data. We must however expect that stripes and chevrons will occur simultaneously in generic transport problems whenever these are characterized by intersecting unidirectional flows while having a sufficiently peaked velocity distribution and a large enough  $g$ .

## REFERENCES

- [1] A. SCHADSCHNEIDER, in: H. UMEO, S. MORISHITA, K. NISHINARI, T. KOMATSUZAKI, S. BANDINI (EDS.), *Cellular automata, Proceedings. Book Series: Lecture Notes in Computer Science*, **5191** (2008) 22–31
- [2] D. HELBING, *Reviews of Modern Physics*, **73** (2001) 1067–1141
- [3] S. P. HOOGENDOORN and W. DAAMEN, in: S. HOOGENDOORN and S. LUDING and P. BOVY, ET AL. (EDS.), *Traffic and Granular Flow '03, Springer*2005, p. 121–132
- [4] S. P. HOOGENDOORN and P. H. L. BOVY, *Simulation of pedestrian flows by optimal control and differential games Optim. Control Appl. Meth.*, **24** (2003) 153–172.
- [5] K. YAMAMOTO and M. OKADA, in: *2011 IEEE International Conference on Robotics and Automation*2011
- [6] O. BIHAM and A. MIDDLETON and D. LEVINE, *Phys. Rev. A*, **46** (1992) R6124–R6127
- [7] H.J. HILHORST and C. APPERT-ROLLAND, *J. Stat. Mech.*, (2012) P06009.
- [8] With the frozen shuffle update of ref. [9] the exact formula is  $J(\alpha) = -\log(1 - \alpha)/[1 - \log(1 - \alpha)]$ .
- [9] C. APPERT-ROLLAND and J. CIVIDINI and H.J. HILHORST, *J. Stat. Mech.*, (2011) P10013
- [10] C. APPERT-ROLLAND and J. CIVIDINI and H.J. HILHORST, *J. Stat. Mech.*, (2011) P07009
- [11] C. APPERT-ROLLAND and J. CIVIDINI and H.J. HILHORST, *J. Stat. Mech.*, (2011) P10014
- [12] H.J. HILHORST and J. CIVIDINI and C. APPERT-ROLLAND, To appear in: *Perspectives and Challenges in Statistical Physics and Complex Systems for the Next Decade (World Scientific, Singapore)* 2013
- [13] J. CIVIDINI and H.J. HILHORST and C. APPERT-ROLLAND, *J. Phys. A: Math. Theor.*, **46** (2013) 345002
- [14] J. CIVIDINI and C. APPERT-ROLLAND, *J. Stat. Mech.*, (2013) P07015